DOI: 10.22630/TPFP.2024.1.10031

ORIGINAL PAPER
Received: 15.10.2024
Accepted: 31.01.2025

SCIENCE AND TECHNOLOGY PARTNERSHIP: APPLICATION OF COMPUTATIONAL FLUID DYNAMICS TO PREDICT THE TURKEY MEAT PROTEIN DENATURATION PROCESS IN THE CONTEXT OF A HEALTHY DIET FOR CHILDREN AND ADOLESCENTS

Arkadiusz SZPICER✉, Weronika BIŃKOWSKA, Adrian STELMASIAK, Magdalena ZALEWSKA, Iwona WOJTASIK-KALINOWSKA, Andrzej PÓŁTORAK

Warsaw University of Life Sciences – SGGW

Abstract: In the current era marked by increased consumer awareness and advancements in food technology, the quality of turkey meat has emerged as a focal point, particularly in promoting healthy diets for children and adolescents. As parents seek nutritious and appealing food options for younger consumers, understanding protein denaturation becomes critical for enhancing meat texture, juiciness, and overall sensory experience. This study explores the application of Computational Fluid Dynamics to predict and optimise the denaturation of turkey meat proteins during thermal processing. By utilising CFD, this research models the heat and mass transfer dynamics involved in cooking turkey meat, providing insights that can optimise the cooking conditions to preserve nutritional value while improving the sensory qualities. The results indicated optimal thermal treatment conditions – 161.28°C, 61.31% humidity, and 17.58 rpm fan speed. Laboratory validations confirmed that the predicted denaturation of myosin and actin aligned closely with experimental results, underscoring the efficacy of CFD as a predictive tool. Moreover, no statistically significant discrepancies were observed in collagen denaturation between the predicted and experimental results ($P > 0.05$), further demonstrating the accuracy of the model. Overall, this work illustrates the potential of CFD in food science, enabling the development of high-quality, safe, and sustainable turkey meat products that fulfil the nutritional needs of children and adolescents.

Key words: Computational Fluid Dynamics (CFD), Protein Denaturation, Turkey Meat Processing, Healthy Diet for Children, Thermal Process Optimisation, Nutritional Quality in Meat

✉ Arkadiusz Szpicer – Department of Technique and Food Development, 02-787 Warszawa, 166 Nowoursynowska St.; e-mail: arkadiusz_szpicer@sggw.edu.pl; https://orcid.org/0000-0001-8817-7342

Weronika Bińkowska – Department of Technique and Food Development, 02-787 Warszawa, 166 Nowoursynowska St.; e-mail: weronika_binkowska@sggw.edu.pl; https://orcid.org/0000-0002-6378-2471

Adrian Stelmasiak – Department of Technique and Food Development, 02-787 Warszawa, 166 Nowoursynowska St.; e-mail: adrian_stelmasiak@sggw.edu.pl; https://orcid.org/0000-0003-0249-6030

Magdalena Zalewska – Department of Technique and Food Development, 02-787 Warszawa, 166 Nowoursynowska St.; e-mail: magdalena_zalewska@sggw.edu.pl; https://orcid.org/0000-0001-8727-6541

Iwona Wojtasik-Kalinowska – Department of Technique and Food Development, 02-787 Warszawa, 166 Nowoursynowska St.; e-mail: iwona_wojtasik-kalinowska@sggw.edu.pl; https://orcid.org/0000-0002-9056-7777

Andrzej Półtorak – Department of Technique and Food Development, 02-787 Warszawa, 166 Nowoursynowska St.; e-mail: andrzej_poltorak@sggw.edu.pl; https://orcid.org/0000-0002-6482-5904

INTRODUCTION

Understanding the quality of turkey meat is crucial for promoting healthy diets, particularly for children and adolescents. Turkey meat is valued for its lean protein content and health benefits, making it a recommended component of balanced diets for younger consumers. However, achieving high standards of nutritional quality, sensory appeal, and safety in turkey meat requires an in-depth understanding of the thermal processes that influence protein denaturation during cooking. This phenomenon significantly impacts the meat texture, juiciness, and overall appeal, which are critical factors in encouraging healthier eating habits [1–3].

Computational Fluid Dynamics (CFD) offers an innovative approach to modelling and optimising the thermal processing of turkey meat. By simulating heat and mass transfer, CFD provides insights into how temperature and cooking time affect protein structure and quality. This technology enables precise control over heat distribution and minimising protein degradation while preserving nutritional value and sensory qualities [4, 5]. Optimising these processes not only ensures high-quality meat products but also aligns with dietary guidelines for children and adolescents by maintaining digestibility and reducing the content of undesirable compounds [6].

CFD also supports sustainability and food safety initiatives. By optimising the cooking conditions, it reduces energy consumption, minimises waste, and ensures uniform cooking, which helps eliminate the risks associated with undercooked meat while maintaining its sensory attributes [7, 8]. These advancements demonstrate the potential of CFD to enhance the quality and healthfulness of turkey meat, contributing to broader goals of promoting sustainable and nutritious food options for younger generations [9, 10].

This study aims to explore the application of CFD in predicting and optimising the denaturation process of turkey meat proteins during thermal processing. It also examines potential benefits of this technology in enhancing food safety, sustainability, and energy efficiency, supporting dietary and environmental objectives.

MATERIAL AND METHODS

The experiment was carried out in several phases:

- in the first step, an experimental model was developed using the Design-Expert program,
- the second phase was a simulation of the heat treatment process using CFD,
- the third stage was roasting optimisation using RSM (response surface methodology),
- the final stage was verification of the predicted results using laboratory tests.

Experiment design

Three design variables – temperature, humidity, and fan rotation speed – were chosen as quantitative independent factors to evaluate their effects on the denaturation levels of myosin, collagen, actin, and cooking loss. These variables were tested in the following ranges: temperature from 120°C to 200°C, humidity from 0% to 75%, and fan rotation speed from 0 to 1,400 rpm. The parameter ranges were established through a combination of literature review and preliminary experiments [4]. To assess the outcomes, the Design-Expert version 11 software (Stat-Ease, Inc., USA) was employed, generating 20 experimental runs (as shown in Table 1). A quadratic equation was used to model the interactions between variables and responses, with the model's central point repeated six times for validation.

Table 1. Experimental design used for CFD simulations

Run	Heat treatment parameters			Run	Heat treatment parameters		
	Temperature [°C]	Humidity [%]	Fan rotation [rpm]		Temperature [°C]	Humidity [%]	Fan rotation [rpm]
1	120	0	0	11	160	0	700
2	200	0	0	12	160	75	700
3	120	75	0	13	160	37.5	0
4	200	75	0	14	160	37.5	1,400
5	120	0	1,400	15 C	160	37.5	700
6	200	0	1,400	16 C	160	37.5	700
7	120	75	1,400	17 C	160	37.5	700
8	200	75	1,400	18 C	160	37.5	700
9	120	37.5	700	19 C	160	37.5	700
10	200	37.5	700	20 C	160	37.5	700

C – central points

Source: own elaboration

Heat treatment process using CDF simulation. CFD Description and Implementation

The Ansys v.19.0 software was utilised to develop a three-dimensional model of the testing apparatus and to simulate the thermal treatment process. This simulation followed the methodology described by Szpicer et al. (2022), with some modifications made for the study [11]. The scheme of the studied system is shown in Figure 1. Key factors affecting the thermal properties of food products include their fundamental composition, which consists of the amounts of protein, fat, carbohydrates, and ash. The conduction coefficient (λ) and specific heat (Cp) of the raw material are critical in determining these properties. The basic composition of turkey breast meat can vary due to factors such as age, developmental stage, and activity levels [12–15]. The thermophysical properties of turkey meat, such as the thermal conductivity (λ), specific heat (Cp), and density, were treated as temperature-dependent variables. These properties were calculated using the equations proposed by Choi and Okos (1986), with adjustments based on the meat's composition. Furthermore, water evaporation during cooking was modelled using Fick's law of diffusion, and its impact on the local thermal conductivity and specific heat was incorporated into the simulation [16].

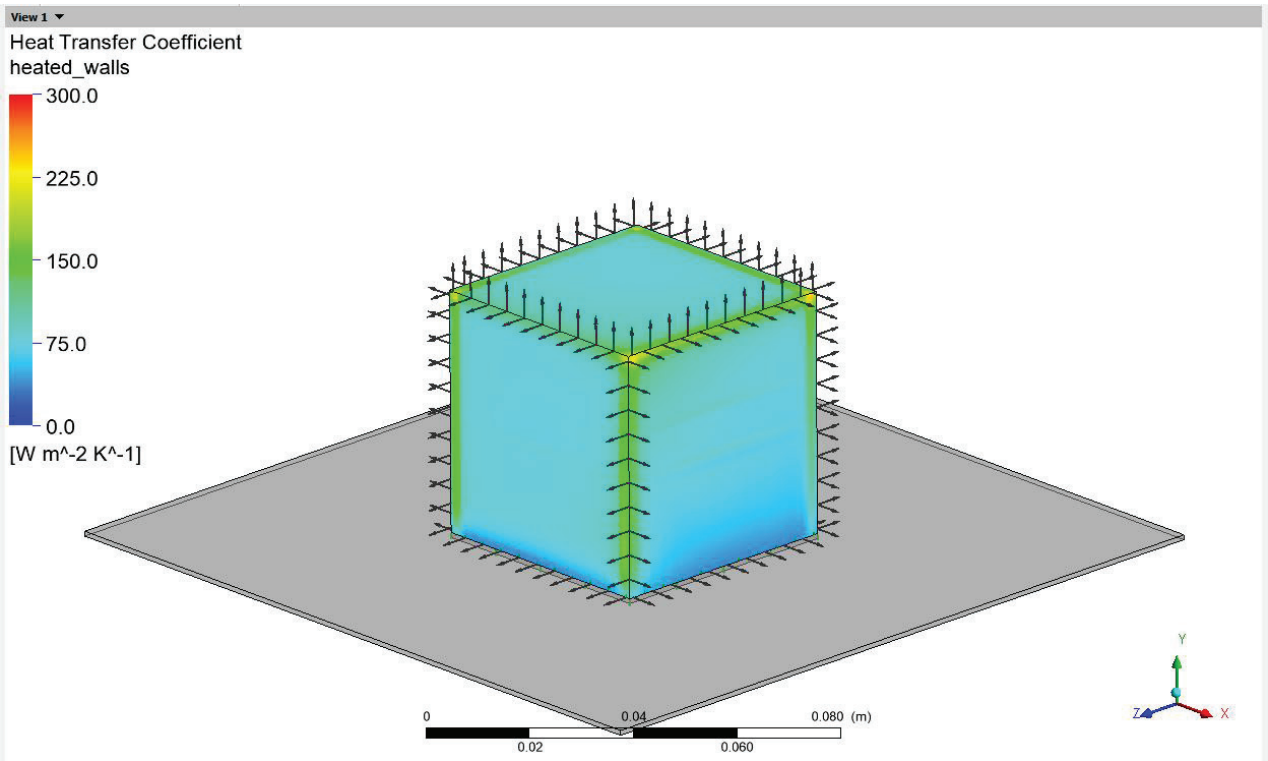

Figure 1. Scheme of the studied system

Source: own elaboration.

For the simulation, input data were sourced from the composition analysis conducted by Gantner et al. (2017), which reported the following values: 77.03 ±0.21% water, 1.98 ±0.49% fat, 19.03 ±0.23% protein, 1.46 ±0.45% connective tissue, and 1.61 ±0.03% ash [17]. The objective of this research was to determine the thermal penetration coefficient to calculate the denaturation extent of individual proteins and the resulting cooking loss. Temperature and enthalpy data for each protein type were gathered using differential scanning calorimetry (DSC): myosin at 61.5°C, collagen at 67°C, and actin at 80.5°C, with corresponding enthalpies of 3.85 J/gK, 3.84 J/gK, and 3.93 J/gK, respectively [15]. For the simulation, a 3D model of a combi steamer (CPE 110, Convect-Air Professional, Küppersbusch, Germany) was created following the methodology specified by Szpicer et al. (2024) [18]. The model incorporated a heat source (heater), fan, steam generator, and GN container rack. A cube of turkey breast meat (50 × 50 × 50 mm) was placed on a GN ½ tray (530 × 325 × 20 mm) inside the oven. The simulated roasting duration was established at 2,000 seconds, assuming the turkey breast meat had a homogeneous microstructure and isotropic properties regarding mass and heat, without accounting for transport and fat loss. The forced convection was characterised by the global heat transfer coefficient, and water diffusion was modelled using Fick's law of diffusion with a global diffusion coefficient. Cooking loss from water squeezing was considered, while thermal contraction and shape changes were neglected, keeping the sample volume constant throughout the roasting process [10, 11 ,19].

NUMERICAL MODEL

Analysed space

The model comprised three distinct domains. The initial domain encompassed the fluid surrounding the sleeve--shaped rotor, which operated at a designated rotational speed. This configuration facilitated the simulation of the rotor's rotation within the chamber, with the blades represented as surfaces. The second domain represented the chamber area where air circulation was induced by the rotating rotor. Lastly, the third domain included two solid components: the sample insert and the support plate.

Mesh

A hexa structural mesh was applied to the rotor space, incorporating surface compaction for the rotor blades to enhance the representation of the flow. For the chamber, a tetra/prism mesh was utilised, with prismatic elements strategically placed, such as along the meat and plate walls, for heat transfer analysis. A hexa mesh was chosen for the turkey breast meat and plate. The model specifications were as follows: rotor space – 152,880 hexes and 177,702 nodes; chamber – 339,867 tetras, 100,385 prisms and 120,714 nodes; meat and plate – 64,372 hexes and 73,325 nodes.

Materials

In the computations, the materials used included a blend of air and water vapour, turkey meat as the used material, and stainless steel (AISI 304). The initial temperature of the solids was set at 23°C.

MATERIAL DATA

Turkey breast meat

The determination of the conduction coefficient (λ) relied on Eq. (1) following the description by Choi and Okos, considering the essential composition of the sample [16].

$$\lambda = 0.205x_c + 0.20x_p + 0.175x_f + 0.135x_a + 0.61x_w \quad (1)$$

where:
x – mass fraction of the food ingredient,
indexes:
c – carbohydrates,
p – proteins,
f – fat,
a – ash,
w – water.

The computation of specific heat (C_p) was derived from Eq. (2) following the explanation provided by Singh and Heldman, considering the fundamental composition of the samples [20].

$$C_p = 1.424x_c + 1.549x_p + 1.675x_f + 0.837x_a + 4.187x_w \quad (2)$$

where:
x – mass fraction of the food ingredient,
indexes:
c – carbohydrates,
p – proteins,
f – fat,
a – ash,
w – water.

Stainless steel (AISI 304)
Conduction coefficient (λ) – 60.5 W/mK
Specific heat (C_p) – 434 J/kgK.
Air – Air Ideal Gas:

The ideal gas equation of state can be applied for the computation of different gas properties according to Eq. (3).

$$pV = nRT \tag{3}$$

where:
p – absolute pressure of the gas,
V – volume of the gas,
n – amount of substance of gas (also known as number of moles),
R – ideal, or universal, gas constant, equal to the product of the Boltzmann constant and the Avogadro constant,
T – absolute temperature of the gas.

Water vapour – Redlich-Kwong Dry Steam:

Pressure and molar volume of dry steam were calculated using the Redlich–Kwong equation (Eq. 4) to accurately model heat and mass transfer conditions in the CFD simulations [21]:

$$p = \frac{RT}{V_m - b} - \frac{a}{\sqrt{T}V_m\left(V_m + b\right)} \tag{4}$$

where:
p – gas pressure,
R – gas constant,
T – temperature,
V_m – molar volume (V/n),
a – constant that corrects for the attractive potential of molecules,
b – constant that corrects for the volume.

The gas used in the experiment was a blend of steam and air, with the mixture's composition determined by the mass fractions of its individual components.

Humidity

$$\log e^* = -7.90298\left(\frac{T_{st}}{T} - 1\right) + 5.02808\log\left(\frac{T_{st}}{T}\right) - 1.3816\times10^{-7}\left(10^{11.344\left(1-\frac{T}{T_{st}}\right)} - 1\right) + 8.1328\times10^{-3}\left(10^{-3.49149\left(\frac{T_{st}}{T}\right)} - 1\right) + \log e^*_{st} \tag{5}$$

where:
log refers to the logarithm in base 10,
e* – saturation water vapour pressure (hPa),
T – absolute air temperature in Kelvins,
T_{st} – steam-point (i.e. boiling point at 1 atm.) temperature (373.15 K),
e^*_{st} – e* at the steam-point pressure (1 atm = 1,013.25 hPa).

Using Eq. (6), the mass fraction of water vapour in the mixture was established by considering the saturation pressure at the provided temperature and the designated humidity.

$$X = 6.222\frac{\phi Ps}{1013.25 + \phi Ps} \tag{6}$$

$$gH_2O = \frac{X}{X+1}$$

Definition of the solver

The SST turbulence model solver parameters were configured with a convergence criterion of 10e-4 and 600 iterations. Before finalising the mesh size and solver parameters, a mesh independence study was conducted to ensure the robustness of the model. Several mesh configurations were tested, gradually increasing the number of elements, while observing the impact on the key output parameters, such as the temperature distribution, heat transfer coefficients, and protein denaturation levels. The selected mesh (152,880 hex elements for the rotor space, 339,867 tetrahedral elements for the chamber, and 64,372 hex elements for the meat and plate) provided a balance between computational cost and accuracy. Further refinement resulted in negligible changes to the output

parameters (<1%). In addition, an adaptive time-stepping approach was configured, with a range of 0.1 to 10 seconds and 2–5 iterations per step. This setup was chosen to address the transient nature of the heat treatment process. Smaller time steps were applied during periods of rapid temperature changes, such as the initial heating phase, while larger steps were used when temperature gradients had stabilised. This approach ensured numerical stability, accurate results, and optimised computational efficiency.

The solver work type was designated as Double Precision. The choice of the Shear Stress Transport (SST) turbulence model was based on its flexibility, effective handling of boundary layers, relatively low computational complexity, and widespread use in the field of CFD. For the transient state solver definition, the adaptive time step was established with 2–5 iterations per step, a time step range of 0.1–10 seconds, and a process duration of 2,000 seconds.

Validation of the Computational Model

In this study, a detailed validation of the Computational Fluid Dynamics (CFD) model was conducted to confirm its reliability in predicting temperature distributions within turkey breast samples during thermal processing. This step was crucial for ensuring the model's ability to accurately simulate protein denaturation, which is driven by temperature changes.

Experimental Setup

To validate the model, turkey breast samples (50 × 50 × 50 mm) were thermally treated in a combi-steam oven (Küppersbusch CPE-110, Germany) at: 160°C, 37.5% humidity, and 1,400 rpm fan speed. Temperature measurements were taken using Type-K thermocouples (Ellab TrackSense Pro, Denmark) placed at three key locations within the sample:

- Core: Geometric centre of the meat cube.
- Midpoint: Halfway between the core and the surface.
- Surface: Outermost layer of the sample.

Measurements were recorded at 10-second intervals over a 2,000-second roasting period. Three biological replicates were conducted to ensure repeatability and reliability.

Predicted and Measured Temperature Comparisons

The CFD model provided temperature predictions at the same locations and time points as the experimental measurements. Table 2 summarises the predicted and experimentally measured temperatures (±*SD*) at 500, 1,000, 1,500, and 2,000 seconds.

Table 2. Validation of the Computational Model

Time [s]	Core temperature [°C]		Midpoint temperature [°C]		Surface temperature [°C]	
	CFD Prediction	Experimental	CFD Prediction	Experimental	CFD Prediction	Experimental
500	42.3 ±1.1	43.0 ±1.4	58.7 ±0.9	57.8 ±1.3	68.2 ±1.2	68.5 ±1.6
1,000	57.5 ±1.3	56.9 ±1.2	69.4 ±1.0	70.2 ±1.5	79.3 ±1.4	78.6 ±1.7
1,500	68.7 ±1.2	68.4 ±1.5	76.3 ±1.1	77.0 ±1.4	85.5 ±1.3	85.1 ±1.8
2,000	74.2 ±1.0	74.5 ±1.3	81.6 ±0.8	81.9 ±1.6	89.1 ±1.5	88.7 ±1.7

Statistical Validation

A Student's t-test was performed to evaluate the differences between the predicted and measured temperatures at each location and time point. The results showed no statistically significant differences ($P > 0.05$) between the predicted and experimental temperatures, confirming the model's accuracy. The maximum observed error was less than 2%, which is within an acceptable range for CFD applications in food processing. The validation results demonstrate that the CFD model provides highly accurate predictions of temperature distributions during thermal treatment. The alignment between the predicted and experimental temperatures at all measured points confirms the model's capability to capture the heat transfer dynamics and their impact on protein denaturation. The core temperature predictions exhibited minimal deviation, with a maximum difference of 0.9°C at 500 seconds. The surface temperature predictions consistently matched the experimental measurements within 0.5°C, indicating precise modelling of boundary heat transfer.

Stages of CFD Analysis

The CFD analysis was conducted in two phases, necessitated by the fluctuating output parameters during heat treatment and the model's size. The initial stage encompassed a steady-state analysis, yielding actual heat transfer coefficients on the surfaces of the meat sample and the GN container. In the subsequent phase, the outcomes from the first stage were used in modelling the solids (meat and GN container), and transient simulations were executed to capture the temperature variations of the samples over time. The initial phase focused on determining penetration coefficients, while the second phase involved simulating protein denaturation and water loss.

Roasting optimisation using RSM

In this experiment, the influence of three factors on the denaturation of myosin, collagen and actin, and mass loss was examined. The variables considered were the temperature within the furnace, air stream speed (fan speed), and humidity level. To interpret and characterise the relationship between these variables and the measured parameters, a quadratic equation was used. The central point was replicated six times in the model. Using Design-Expert version 11 (Stat-Ease, Inc., USA), the heat treatment was optimised concerning the denaturation of myosin, collagen and actin, and the cooking loss based on the model. The final step involved optimising the thermal treatment parameters using a mathematical model and experimental validation of the calculated response values.

Verification of the predicted results using laboratory tests

Materials

Turkey breast fillets (*Pectoralis major*) for analysis were obtained from a BIG 6 turkey acquired from a commercial market (INDYKPOL S.A., Olsztyn, Poland). The fillets were taken for further processing (1,954 ±174 g). The fillets were transported to the laboratory in cooling boxes, maintaining chilled conditions at 4±1°C. Cube-shaped samples (50 × 50 × 50 mm) were cut from turkey breasts according to Figure 2.

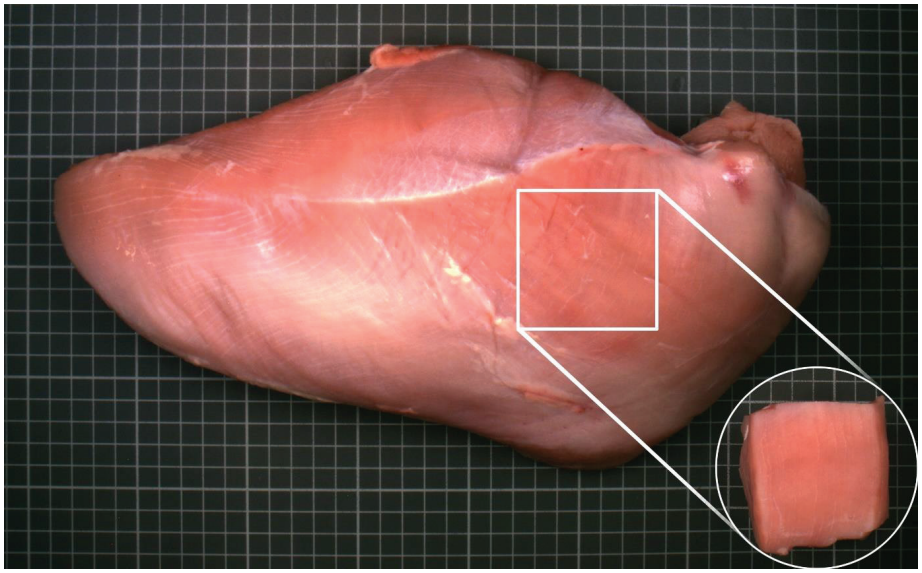

Figure 2. Preparation of turkey sample (50 × 50 × 50 mm) from breast fillets (Pectoralis major) for verification stage

Source: own elaboration.

Basic composition evaluation

The basic composition of turkey breast meat samples was evaluated using the near-infrared (NIR) spectrometry method as outlined by Stelmasiak et al. (2019) [22]. The analysis was conducted using a NIRFlex N-500 spectrometer with a solids module (Büchi Labortechnik AG, Switzerland) in reflectance mode, covering a spectral range of 12,500–4,000 cm^{-1}, and using a Büchi Art. N. N555-501. This analysis occurred at an accredited NIR laboratory (Polish Centre for Accreditation FT-NIR – Accreditation No. AB 1670). Homogenised meat samples, each weighing 100 g, were placed on a Petri dish and subjected to measurements. The assessment of the basic composition, encompassing water, fat, proteins, CTP (collagen protein total) and ash, was conducted in triplicate for each sample to ensure the precision and reliability of the results (three technical replications). Measurements were taken for each of the three independent biological replications (three different batches) involving distinct raw materials.

Heat treatment

The turkey meat cubes were thermally processed in accordance with the optimised parameters based on RSM data in a Küppersbusch CPE-110 combi-steam oven (Küppersbusch Convect-Air Professional, Germany). The process parameters were controlled using wireless temperature and humidity recorders (TrackSense Pro; Ellab, Denmark).

Protein denaturation level

Protein denaturation levels were assessed through differential scanning calorimetry (DSC 1 from Mettler Toledo, Schwerzenbach, Switzerland) [11]. Prior to the experiment, the device underwent calibration with pure zinc and indium. Both untreated and heat-treated samples were examined. A BÜCHI B-400 homogeniser was used for the uniform mixing of each sample. Subsequently, 10.0 ±0.1 mg of meat samples were deposited into a standard 40 µl aluminium pan (No.: ME-51119870) and hermetically sealed with an aluminium lid (No.: ME-51119871) using a Mettler Toledo Crucible Sealing Press.

Under an argon atmosphere (100 cm^3/min), the DSC analysis was conducted at a rate of 10°C/min (β) within the temperature range of 10°C to 100°C. The resultant thermograms were scrutinised using the STARe software to identify the initial (T_{on}), maximum (T_{max}), and final (T_{end}) temperatures, along with the enthalpy (ΔH). The degree of denaturation for myosin, collagen, and actin was ascertained based on the thermograms, using the methodology outlined by Agafonkina et al. (2019) [15]. The denaturation percentage for each protein was calculated by comparing the enthalpy of denaturation between the untreated and heat-treated samples, using equation (7).

$$\text{Denaturation } \% = \frac{H_{raw} - H_{roasted}}{H_{raw}} \times 100 \quad (7)$$

where:
H_{raw} – enthalpy of protein denaturation in raw meat prior to heat treatment (J/g),
$H_{roasted}$ – enthalpy of protein denaturation in roasted meat following heat treatment (J/g).

The evaluation of the degree of denaturation was conducted thrice for each sample to assure the precision and dependability of the outcomes (three technical replicates). Measurements were carried out across three independent biological replicates (three separate batches) using distinct raw materials for each.

Protein Denaturation Modelling Based on Temperature Predictions

To establish the connection between the temperature predictions from the Computational Fluid Dynamics (CFD) simulations and the extent of protein denaturation in the turkey breast meat, a detailed modelling approach was implemented. This section describes the methodology used to calculate the protein denaturation based on spatial and temporal temperature distributions.

Temperature Thresholds for Protein Denaturation

The Differential Scanning Calorimetry (DSC) data were used to identify the denaturation thresholds for the primary proteins in the turkey meat. The specific denaturation temperatures (±*SD*) and enthalpy values (ΔH) used in the model were as follows (Table 3):

Table 3. Denaturation thresholds and enthalpy changes (ΔH) for key turkey meat proteins

Protein	Denaturation Onset [T, °C]	Enthalpy Change [ΔH, J/g]
Myosin	61.5 ±0.8	3.85 ±0.12
Collagen	67.0 ±0.1	3.84 ±0.15
Actin	80.5 ±0.9	3.93 ±0.10

Source: own elaboration.

These thresholds represent critical points at which the respective proteins undergo irreversible structural changes, impacting the texture and functionality. The enthalpy data were integrated into kinetic equations to model the protein denaturation.

Spatial and Temporal Modelling of Protein Denaturation

1. Temperature Data from CFD Simulations:
   - The CFD model provided a three-dimensional grid of the turkey meat sample, with each grid element representing a localised region.
   - For each grid element, the transient temperature profile was extracted over the simulated roasting period (2,000 seconds).
2. Kinetic Model for Protein Denaturation:
   - Protein denaturation was modelled using a first-order kinetic equation:

$$\frac{d\alpha}{dt} = k(T)\cdot(1-\alpha)$$

where:
$\alpha(t)$ – degree of denaturation at time t,
$k(T)$ – temperature-dependent rate constant, calculated using the Arrhenius equation:

$$k(T) = A\cdot e^{\frac{-E_a}{RT}}$$

with:
A – pre-exponential factor [1/s],
Ea – activation energy [J/mol],
R – universal gas constant (8.314 J/mol·K),
T – absolute temperature [K].

3. Spatial Variation in Denaturation:
   - Using the temperature data for each grid element, the degree of denaturation was calculated iteratively for each time step.
   - The enthalpy changes (ΔH) associated with each protein were incorporated into the calculations to adjust for localised thermal effects.
   - The resulting denaturation values were mapped across the 3D grid to visualise the spatial variation of protein denaturation within the meat sample.
4. Aggregation of Results:
   - The overall denaturation of each protein was determined by integrating the localised denaturation values across the entire sample. This approach ensured that spatial heterogeneity in heat transfer and protein response was accounted for.

Validation of Predicted Denaturation

Laboratory experiments were conducted to validate the predicted protein denaturation levels. Differential Scanning Calorimetry (DSC) was employed to measure the actual denaturation percentages for myosin, collagen, and actin in the samples subjected to the optimised roasting parameters. Table 4 compares the predicted and experimental results for protein denaturation and cooking loss:

Table 4. Comparison of CFD-predicted and experimentally measured protein denaturation and cooking loss

Parameter	Predicted value [±SD]	Experimental value [±SD]	P-value
Myosin Denaturation [%]	99.41 ±1.03	99.18 ±0.72	>0.05
Collagen denaturation [%]	88.37 ±1.02	87.67 ±0.75	>0.05
Actin denaturation [%]	20.70 ±0.78	19.21 ±0.32	>0.05

Source: own elaboration.

The predicted values from the CFD model showed strong agreement with the experimental results, with no statistically significant differences ($P > 0.05$) for all parameters. These results confirm the reliability of the model in predicting protein denaturation and cooking loss during thermal processing.

Cooking Loss

For the assessment of cooking loss, the sample underwent weighing before entering the oven and promptly after extraction. The percentage of cooking loss was computed by evaluating the disparity in mass between the raw and heat-treated meat using Equation (8).

$$\text{Cooking loss}\% = \frac{(M_{raw} - M_{roasted})}{M_{raw}} \times 100 \quad (8)$$

where:
M_{raw} – mass of the raw sample prior to heat treatment (g),
$M_{roasted}$ – mass of the roasted sample following heat treatment (g).

The evaluation of the cooking loss was conducted three times for each sample to guarantee the accuracy and reliability of the findings (three technical replicates). Measurements were carried out across three independent biological replicates (three distinct batches), using varied raw materials for each batch.

Statistics

The experimental design was executed using the Design-Expert v. 11 software (Stat-Ease, Inc., USA), as outlined in Table 1. An examination of the impact of temperature, humidity, and convection intensity on individual responses was conducted following the programmed experimental model. The significant terms within this model were identified through analysis of variance (ANOVA) for each response, assessing a lack of fit, coefficients of determination (R^2), and coefficients of variation (CV) to ensure model accuracy. 3D charts were constructed based on the analysis results, and quadratic equations describing the model were used for further studies.

In the prediction analysis using RSM, the maximum desirable degree of myosin and collagen denaturation was determined, with the minimisation of actin denaturation and mass loss selected as parameters.

The final stage of the experiment involved optimising and validating the heat treatment technology. Predicted response values were then compared with experimentally determined values. Instrumental technique analyses were conducted using raw materials from various production batches in three independent biological replicates. Following optimisation, Student's *t*-test at $P \leq 0.05$ was applied to ascertain differences between two sets of values: predicted and measured properties in the laboratory experiments. Statistical analyses were performed using the Design-Expert software, and the results were presented as mean ($\bar{X}$) ± standard error (SD).

RESULTS AND DISCUSSION

Table 5 summarises the regression coefficients of the quadratic polynomial models predicting myosin, collagen and actin denaturation, and cooking loss. The models exhibited high adequacy (R^2 = 0.746–0.997). Myosin, collagen, and actin denaturation achieved the highest R^2 values (0.933, 0.984, 0.997), while cooking loss was the least predictive (R^2 = 0.746). Finding all lack-of-fit p-values confirmed satisfactory model fits (p >0.05).

Table 5. Regression coefficients of the predicted quadratic polynomial models for the physical values of the of myosin, collagen and actin denaturation, and cooking loss.

Factor	Denatured myosin [%]	Denatured collagen [%]	Denatured actin [%]	Cooking loss [%]
Intercept	96.27	86.39	17.76	20.32
Temp	2.71***	17.00***	24.01***	2.96**
Hum	2.68***	3.71***	6.20***	0.26
Fan	1.12*	1.71*	4.12***	2.18*
Temp × Hum	−2.56***	−1.40	2.66*	−0.10
Temp × Fan	−0.66	−1.00	3.31***	−0.75
Hum × Fan	−0.56	−0.23	−2.76*	−0.10
$Temp^2$	−0.38	−7.75***	26.44***	0.67
Hum^2	−0.63	0.40	−1.31	0.37
Fan^2	0.56	1.00	0.89	−0.43
R^2	0.933	0.984	0.997	0.746
Lack of fit	0.261	0.289	0.281	0.081

Temp – Temperature, Hum – Humidity, Fan – Fan rotation speed, R^2 – square coefficient of the fitting model, Lack of fit – p-value of lack of fit.
* – Significant at $P \leq 0.05$; ** – Significant at $P \leq 0.01$; *** – Significant at $P \leq 0.001$.

Source: own elaboration.

Optimisation of heat treatment parameters

RSM was used to assess the influence of temperature, humidity, and fan speed on the heat treatment of turkey breast fillets (*Pectoralis major*). This modelling technique made it possible to observe trends in the outcomes as the independent variables were altered. The regression coefficients outlined in Table 5, along with the 3D plots depicted in Figures 3 and 4, demonstrated that all three independent variables exerted a statistically significant effect on the denaturation levels of individual proteins, encompassing myosin, collagen, actin, and cooking loss in the meat samples. However, the extent of this impact varied depending on the specific response and the level of the independent variable.

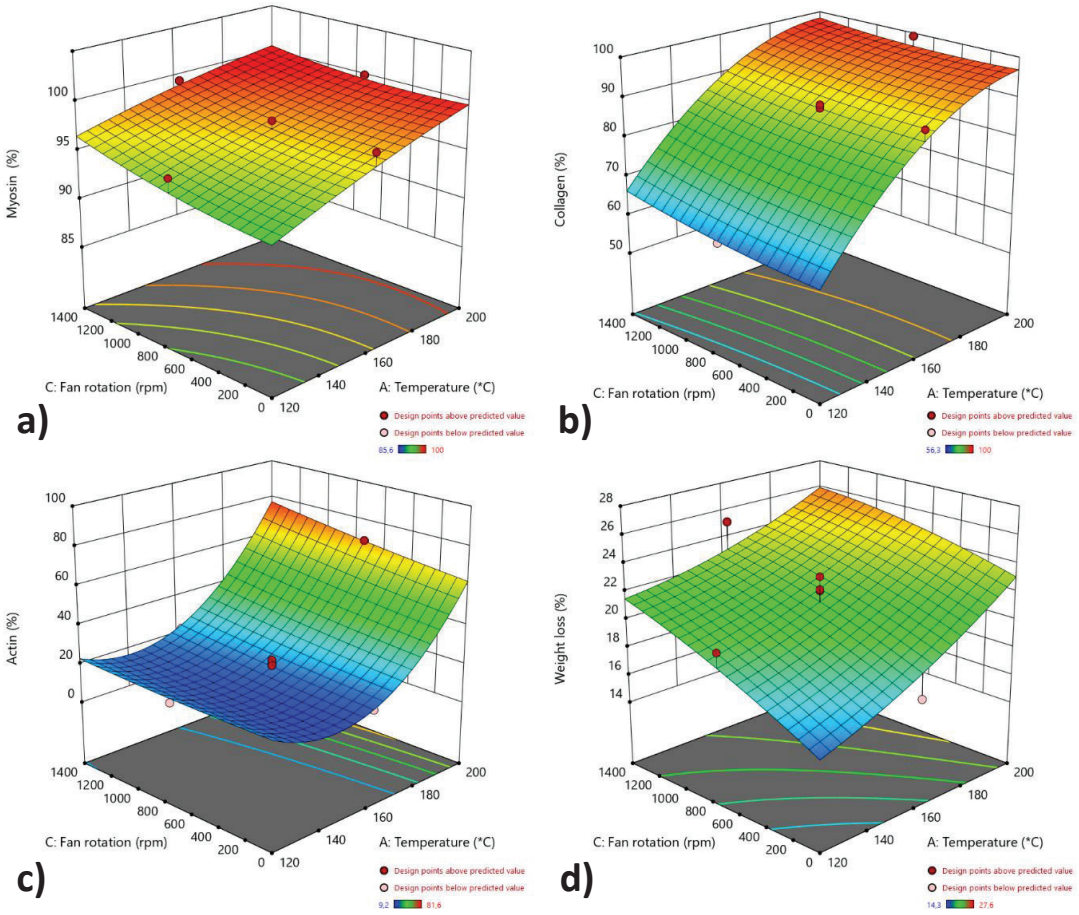

Figure 3. 3D surface charts generated using the RSM model at a humidity of 37.5% illustrate the impact of factors and their interactions on output data: a – myoglobin denaturation [%], b – collagen denaturation [%], c – actin denaturation [%], and d – cooking loss [%]

Source: own elaboration.

The degree of myosin denaturation was significantly influenced by temperature and humidity in linear terms ($P \leq 0.001$), with a similar linear effect observed for fan rotation speed ($P \leq 0.05$). However, quadratic effects of these parameters were not significant ($P > 0.05$), nor were the interactions involving fan speed with temperature or humidity ($P > 0.05$). The strong linear relationship between temperature and myosin denaturation aligns with previous studies, indicating that muscle proteins, including myosin, are highly sensitive to heat. High temperatures disrupt hydrogen and hydrophobic bonds, leading to structural changes that impact protein functionality and digestibility [23]. Similarly, the role of humidity in accelerating denaturation highlights the need for precise humidity control during thermal processing to maintain optimal texture and nutritional quality [24]. The observed linear effect of fan speed suggests that enhanced air circulation facilitates heat transfer and protein denaturation by promoting water evaporation from the meat's surface [25]. The significant interaction between temperature and humidity ($P \leq 0.001$) underscores the necessity of balancing these factors, as low humidity combined with high temperatures can adversely affect meat quality [26]. These findings confirm that the primary factors influencing myosin denaturation operate in a linear fashion, with a limited impact of more complex interactions.

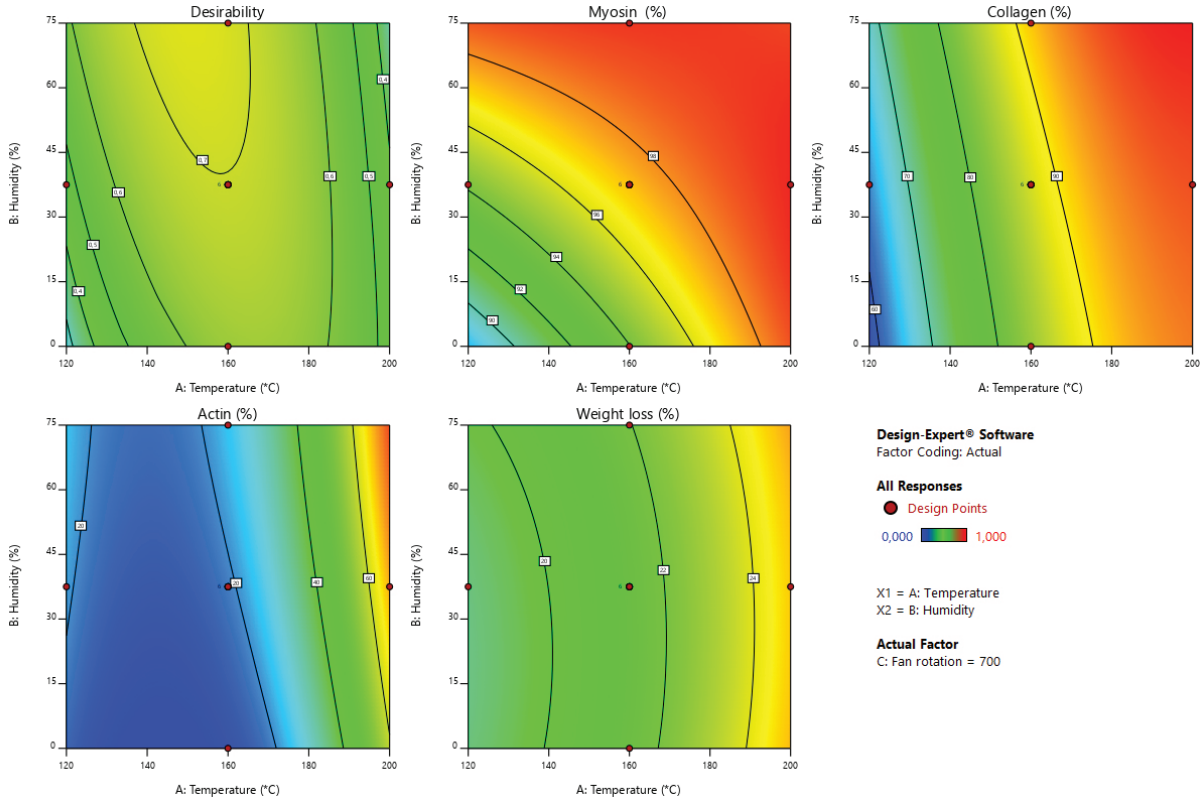

Figure 4. Desirability plots and contour graphic solutions of RSM optimisation

Source: own elaboration.

The investigation into collagen denaturation in turkey breast fillets revealed that temperature, humidity, and fan rotation speed significantly influenced collagen denaturation in linear terms ($P \leq 0.001$, $P \leq 0.001$, $P \leq 0.05$, respectively). Among these, temperature emerged as the most critical factor, with both significant linear and quadratic effects ($P \leq 0.001$). Conversely, humidity and air movement speed did not exhibit statistically significant quadratic effects ($P > 0.05$). Interaction effects between temperature × fan rotation speed, temperature × humidity, and humidity × fan rotation speed were also not statistically significant ($P > 0.05$). These findings align with previous studies on myosin denaturation and other muscle proteins, emphasising temperature as the primary driver of protein denaturation. For instance, computational fluid dynamics (CFD) simulations in pork and beef confirm temperature's dominant role, while humidity and airflow typically play secondary roles [10, 15]. The quadratic effect of temperature reflects the non-linear progression of denaturation at higher temperatures, where collagen breakdown becomes more pronounced. Similar trends have been reported in studies on other meats, such as Atlantic salmon, where environmental factors like air circulation showed limited interactive effects compared to temperature [18]. The results underscore the importance of precise temperature control during meat processing, especially for products intended for children and adolescents, where maintaining protein integrity and nutrient retention is critical for a healthy diet.

All the analysed factors – temperature, humidity, and fan rotation speed – exhibited statistically significant effects on actin denaturation in linear terms ($P \leq 0.001$). Interactions among these factors, such as temperature × × humidity and temperature × fan rotation speed, also had significant impacts ($P \leq 0.05$, $P \leq 0.001$, respectively). However, humidity and fan speed did not show significant quadratic effects ($P > 0.05$), whereas temperature did ($P \leq 0.001$). Temperature emerged as the most critical parameter, influencing actin denaturation both linearly and quadratically ($P \leq 0.001$). Actin, a heat-sensitive protein, begins denaturing around 66°C, with further increases in temperature accelerating the process, as confirmed by CFD simulations and studies on other meats. Elevated temperatures drive moisture loss and textural changes, aligning with findings on pork loin and other muscle foods [10]. Humidity significantly impacted actin denaturation in linear terms, likely due to its role in moisture retention within the meat matrix. Although its quadratic effects were negligible, maintaining optimal humidity is essential to balance moisture retention with heat for effective denaturation. Fan speed influenced denaturation indirectly, primarily through enhanced heat distribution, as shown in the CFD models. However, its effects plateau beyond

certain levels, reflecting findings from similar studies [27, 28]. In summary, temperature dominates the dynamics of actin denaturation in turkey meat, with humidity and fan speed playing secondary but complementary roles, particularly in linear interactions.

The study investigated how temperature, fan speed, and humidity influence cooking loss during the roasting of turkey breast fillets. Temperature and fan speed significantly affected cooking loss in a linear manner ($P \leq 0.01$ and $P \leq 0.05$, respectively), while chamber humidity showed no significant effect ($P > 0.05$). No significant interaction effects between temperature, fan speed, and humidity were observed, nor were there significant quadratic effects for any factor ($P > 0.05$). Temperature emerged as the dominant factor influencing cooking loss, aligning with established research indicating that higher temperatures expedite protein denaturation and collagen shrinkage, leading to increased water release and weight loss [29]. Similarly, fan speed's significant but smaller effect was attributed to enhanced surface evaporation, which is consistent with studies demonstrating the role of air velocity in drying rates [30]. Interestingly, the lack of a significant impact of humidity ($P > 0.05$) on cooking loss is contrary to findings in certain studies, where high humidity environments during roasting have been reported to slow down moisture evaporation and reduce overall weight loss [31]. Contrary to some findings, humidity did not mitigate weight loss under the tested conditions, possibly due to the specific temperature and fan speed settings. These results reinforce the importance of temperature and air circulation in optimising roasting conditions to minimise cooking loss while maintaining product quality. Prior studies, such as those by Bıyıklı et al. and Gál et al. [23, 32], corroborate that processing temperature and time influence the weight loss, texture, and sensory properties. For example, higher temperatures paired with shorter processing times were associated with lower weight losses and improved sensory qualities, highlighting the interplay between the thermal conditions and meat characteristics. These findings provide valuable insights for designing healthier cooking methods tailored for children and adolescents [23, 32].

VERIFICATION OF HEAT TREATMENT PARAMETERS

The final step of the experiment involved validating the results of the RSM model by comparing them with laboratory tests. The maximal desirable denaturation of myosin and collagen was determined, while actin denaturation and mass loss were minimised. According to the RSM optimisation model, the ideal processing conditions for turkey breast meat are a temperature of 161.28°C, humidity of 61.31%, and a fan speed set at 17.58 rpm. The predicted values for the output parameters ($\bar{X}$ ±SD) were as follows: myosin denaturation at 99.41 ±1.03%, collagen denaturation at 88.37 ±1.02%, actin denaturation at 20.70 ±0.78%, and cooking loss at 18.93 ±0.13%. The results of the optimisation and verification process are presented in Table 6, indicating that the laboratory test outcomes were consistent with the predictions of the RSM model. There were no statistically significant differences observed between the predicted and laboratory test values.

Table 6. Verification of the RSM model with laboratory tests ($\bar{X} \pm SD$)

Design factors	Optimum heat treatment parameters	
Temperature [°C]	161.28	
Humidity [%]	61.31	
Fan rotation [RPM]	17.58	
Responses	Predicted values	Laboratory tests values
Myosin denaturation [%]	99.41 ±1.03	99.18 ±0.72
Collagen denaturation [%]	88.37 ±1.02	87.67 ±0.75
Actin denaturation [%]	20.70 ±0.78	19.21 ±0.32
Weight loss [%]	18.93 ±0.13	16.24 ±0.15

*Letters (A, B) show the significant differences between predicted and laboratory tests values ($P \leq 0.05$).

Source: own elaboration.

CONCLUSIONS AND FUTURE PERSPECTIVES

The work presents the innovative use of the CFD method to predict protein denaturation in turkey breast meat and optimise heat treatment processes. Using mathematical models, the optimal thermal treatment conditions were determined, which were 161.28°C, 61.31% air humidity, and the fan speed set at 17.58 rpm. The denaturation of various proteins and losses during the baking process was assessed. During the verification of the laboratory

results, it was found that the denaturation of myosin and actin, as well as the losses during the cooking process, did not differ significantly from the values predicted on the basis of the response surface model developed based on simulation data. The study proves that the CFD method can be a valuable tool for predicting protein denaturation and losses in the cooking process of turkey breast meat, which can improve the quality and efficiency of products in the food industry.

Acknowledgements
Research financed by the Polish Ministry of Science and Higher Education within funds of Faculty of Human Nutrition and Consumer Sciences, Warsaw University of Life Sciences (WULS), for scientific research.

REFERENCES

[1] **Chauhan A., Kaur H., Yadav S., Jakhar S.K. 2020.** A Hybrid Model for Investigating and Selecting a Sustainable Supply Chain for Agri-Produce in India. Annals of Operations Research 290: 621–642. https://www.doi.org/10.1007/s10479-019-03190-6

[2] **Liu Y., Wang Z., Zhang D., Pan T., Liu H., Shen Q., Hui T. 2022.** Effect of Protein Thermal Denaturation on the Texture Profile Evolution of Beijing Roast Duck. Foods 11: 1–14. https://www.doi.org/10.3390/foods11050664

[3] **Khalid W., Maggiolino A., Kour J., Arshad M.S., Aslam N., Afzal M.F., Meghwar P., Zafar K.U.W., De Palo P., Korma S.A. 2023.** Dynamic Alterations in Protein, Sensory, Chemical, and Oxidative Properties Occurring in Meat during Thermal and Non-Thermal Processing Techniques: A Comprehensive Review. Frontiers in Nutrition 9: 1–19. https://www.doi.org/10.3389/fnut.2022.1057457

[4] **Szpicer A., Bińkowska W., Stelmasiak A., Zalewska M., Wojtasik-Kalinowska I., Piwowarski K., Półtorak A. 2024.** Innovative Implementation of Computational Fluid Dynamics in Proteins Denaturation Process Prediction in Goose Breast Meat and Heat Treatment Processes Optimization. Applied Sciences 14: 1–22. https://www.doi.org/0.3390/app14135567

[5] **De Albuquerque C.D., Curet S., Boillereaux L. 2019.** A 3D-CFD-Heat-Transfer-Based Model for the Microbial Inactivation of Pasteurized Food Products. Innovative Food Science & Emerging Technologies 54: 172–181. https://www.doi.org/10.1016/j.ifset.2019.04.007

[6] **Norton T., Sun D.W. 2006.** Computational Fluid Dynamics (CFD) – an Effective and Efficient Design and Analysis Tool for the Food Industry: A Review. Trends in Food Science & Technology 17: 600–620. https://www.doi.org/10.1016/j.tifs.2006.05.004

[7] **James C., Vincent C., de Andrade Lima T.I., James S.J. 2006.** The Primary Chilling of Poultry Carcasses. A Review. International Journal of Refrigeration 29: 847–862. https://www.doi.org/10.1016/j.ijrefrig.2005.08.003

[8] **Park H.W., Yoon W.B. 2018.** Computational Fluid Dynamics (CFD) Modelling and Application for Sterilization of Foods: A Review. Processes 6: 1–14. https://www.doi.org/10.3390/pr6060062

[9] **Szpicer A., Binkowska W., Stelmasiak A., Wojtasik-Kalinowska I., Wierzbicka A., Poltorak A. 2023.** Application of Computational Fluid Dynamics Simulation in Predicting Food Protein Denaturation : Numerical Studies on Selected Food Products. A Review. Animal Science Papers and Reports 41: 307–332. https://www.doi.org/10.2478/aspr-2023-0014.

[10] **Szpicer A., Binkowska W., Wojtasik-Kalinowska I., Półtorak A. 2023.** Prediction of Protein Denaturation and Weight Loss in Pork Loin (Muscle Longissimus Dorsi) Using Computational Fluid Dynamics. European Food Research and Technology 249: 3055–3068. https://www.doi.org/10.1007/s00217-023-04348-0

[11] **Szpicer A., Wierzbicka A., Półtorak A. 2022.** Optimization of Beef Heat Treatment Using CFD Simulation: Modeling of Protein Denaturation Degree. Journal of Food Process Engineering 45: e14014. https://www.doi.org/10.1111/jfpe.14014

[12] **Zielbauer B.I., Franz J., Viezens B., Vilgis T.A. 2016.** Physical Aspects of Meat Cooking: Time Dependent Thermal Protein Denaturation and Water Loss. Food Biophysics 11: 34–42. https://www.doi.org/10.1007/s11483-015-9410-7

[13] **Hassoun A., Aït-Kaddour A., Sahar A., Cozzolino D. 2021.** Monitoring Thermal Treatments Applied to Meat Using Traditional Methods and Spectroscopic Techniques: A Review of Advances over the Last Decade. Food and Bioprocess Technology 14: 195–208. https://www.doi.org/10.1007/s11947-020-02510-0

[14] **Latorre M.E., Palacio M.I., Velázquez D.E., Purslow P.P. 2019.** Specific Effects on Strength and Heat Stability of Intramuscular Connective Tissue during Long Time Low Temperature Cooking. Meat Science 153: 109–116. https://www.doi.org/10.1016/j.meatsci.2019.03.016.

[15] **Agafonkina I.V., Korolev I.A., Sarantsev T.A. 2019.** The Study of Thermal Denaturation of Beef, Pork, Chicken and Turkey Muscle Proteins Using Differential Scanning Calorimetry. Theory and Practice of Meat Processing 4: 19–23. https://www.doi.org/10.21323/2414-438x-2019-4-3-19-23.

[16] **Choi Y., Okos M.R. 1986.** Thermal Properties of Liquid Foods – Review. American Society of Association Executives. 35–77.

[17] **Gantner M., Guzek D., Najda A., Brodowska M., Górska-Horczyczak E., Wojtasik-Kalinowska, I., Godziszewska J. 2017.** Oxidative and Microbial Stability of Poultry Meatballs Added with Coriander Extracts and Packed in Cold Modified Atmosphere. International Journal of Food Properties 20: 2527–2537. https://www.doi.org/10.1080/10942912.2016.1243125

[18] **Szpicer A., Binkowska W., Wojtasik-Kalinowska I., Stelmasiak A., Poltorak A. 2024.** Hybrid Method for Predicting Protein Denaturation and Docosahexaenoic Acid Decomposition in Atlantic Salmon (*Salmo Salar* L.) Using Computational Fluid Dynamics and Response Surface Methodology. European Food Research and Technology 250, 4: 1–14. https://www.doi.org/10.1007/s00217-023-04453-0

[19] **Srikiatden J., Roberts J.S. 2007.** Moisture Transfer in Solid Food Materials: A Review of Mechanisms, Models, and Measurements. International Journal of Food Properties 10: 739–777. https://www.doi.org/10.1080/10942910601161672

[20] **Singh R.P., Heldman D.R. 2014.** Introduction to Food Engineering: Fifth Edition. Elsevier, London.

[21] **Markočič E., Knez Ž. 2016.** Redlich-Kwong Equation of State for Modelling the Solubility of Methane in Water over a Wide Range of Pressures and Temperatures. Fluid Phase Equilibria 408 108–114. https://www.doi.org/10.1016/j.fluid.2015.08.021

[22] **Stelmasiak A., Wyrwisz J., Wierzbicka A. 2019.** Effect of Packaging Methods on Salt-Reduced Smoked-Steamed Ham Using Herbal Extracts. CyTA – Journal of Food 17: 834–840. https://www.doi.org/10.1080/19476337.2019.1660409

[23] **Gál R., Kameník J., Salek R.N., Polášek Z., Macharáčková B., Valenta T., Haruštiaková D., Vinter Š. 2022.** Research Note: Impact of Applied Thermal Treatment on Textural, and Sensory Properties and Cooking Loss of Selected Chicken and Turkey Cuts as Affected by Cooking Technique. Poultry Science 101: 1–6. https://www.doi.org/10.1016/j.psj.2022.101923

[24] **Zhang Y., Dong L., Zhang J., Shi J., Wang Y., Wang S. 2021.** Adverse Effects of Thermal Food Processing on the Structural, Nutritional, and Biological Properties of Proteins. Annual Review of Food Science and Technology 12: 259–286. https://www.doi.org/10.1146/annurev-food-062320-012215

[25] **Desmond E. 2006.** Reducing Salt: A Challenge for the Meat Industry. Meat Science 74: 188–196. https://www.doi.org/10.1016/j.meatsci.2006.04.014

[26] **Kim Y.H.B., Warner R.D., Rosenvold K. 2014.** Influence of High Pre-Rigor Temperature and Fast PH Fall on Muscle Proteins and Meat Quality: A Review. Animal Production Science 54: 375–395. https://www.doi.org/10.1071/AN13329

[27] **Abraha B., Admassu H., Mahmud A., Tsighe N., Shui X.W., Fang Y. 2018.** Effect of Processing Methods on Nutritional and Physico-Chemical Composition of Fish: A Review. MOJ Food Processing & Technology 6: 376–382. https://www.doi.org/10.15406/mojfpt.2018.06.00191

[28] **Yesiltas B., García-Moreno P.J., Sørensen A.D.M., Akoh C.C., Jacobsen C. 2019.** Physical and Oxidative Stability of High Fat Fish Oil-in-Water Emulsions Stabilized with Sodium Caseinate and Phosphatidylcholine as Emulsifiers. Food Chemistry 276: 110–118. https://www.doi.org/10.1016/j.foodchem.2018.09.172

[29] **Tornberg E. 2005.** Effects of Heat on Meat Proteins – Implications on Structure and Quality of Meat Products. Meat Scince 70: 493–508. https://www.doi.org/10.1016/j.meatsci.2004.11.021

[30] **Murphy R.Y., Johnson E.R., Duncan L.K., Clausen E.C., Davis M.D., March J.A. 2001.** Heat Transfer Properties, Moisture Loss, Product Yield, and Soluble Proteins in Chicken Breast Patties during Air Convection Cooking. Poultry Science 80: 508–514. https://www.doi.org/10.1093/ps/80.4.508

[31] **Suleman R., Wang Z., Aadil R.M., Hui T., Hopkins D.L., Zhang D. 2020.** Effect of Cooking on the Nutritive Quality, Sensory Properties and Safety of Lamb Meat: Current Challenges and Future Prospects. Meat Science 167: 108172. https://www.doi.org/10.1016/j.meatsci.2020.108172

[32] **Bıyıklı M., Akoğlu A., Kurhan Ş., Akoğlu İ.T. 2020.** Effect of Different Sous Vide Cooking Temperature-Time Combinations on the Physicochemical, Microbiological, and Sensory Properties of Turkey Cutlet. International Journal of Gastronomy and Food Science 20: 100204. https://www.doi.org/10.1016/j.ijgfs.2020.100204